

UDC 533.661:534.836.2

doi: 10.32620/akt.2023.4.05

Petro LUKIANOV, Oleg DUSHEBA

*National Technical University of Ukraine**“Igor Sikorsky Kyiv Polytechnic Institute”, Kyiv, Ukraine***MODELING OF AERODYNAMIC NOISE OF QUADROTOR TYPE AEROTAXI**

The subject of this work is a study of the current state of modeling the flow around the blades of quadcopters, models of aerodynamic sound generation, formulation, and numerical solution of the problem of generation of rotation noise by the blades of a quadrotor type aerotaxi. The models describing the flow field around the quadrotor blades include the model of nonlinear vortices in lattices, the Reynolds-averaged Navier-Stokes equation (RANS, URANS), the large eddy simulation method (LES), and the direct numerical simulation (DNS) of the system of aerodynamic equations. This paper analyzes the main noise models of different types of aerodynamic origin. Gutin's model is used to describe the noise of the quadrotor rotation, and the Ffowcs - Williams-Hawkins equation in the formulation of Farassat is used to model the noise taking into account various sound sources. However, these approaches have certain drawbacks that limit their application. The following paper uses a modern approach to modeling noise of aerodynamic origin based on the three-dimensional unsteady equation of sound propagation from a thin blade in the potential approximation, previously proposed by one of the authors of the work. Using this approach, a numerical calculation of the problem of sound generation (rotational noise) of the aerodynamic origin of a quadrotor type aerotaxi was performed. **The purpose of the study.** Despite the approaches described above, there is a problem associated with achieving an acceptable noise level, i.e. its further reduction. To solve this problem, there is a need to use more accurate models that will allow research on reducing air taxi noise. **Tasks of the study.** In this regard, the task of modeling noise of aerodynamic origin was set and solved using a refined model of the sound generated by the interaction of the flow and air taxi blades. **Research methods are based on** the construction and use of a mathematical model for the generation of rotation sound generated by the joint operation of aerotaxi rotors. On this basis, the calculations of the near and far sound fields were performed. A new model for calculating the long-range sound field of a quadrotor type aerotaxi is proposed, which considers the mutual formation of the resulting sound field from the joint operation of 4 propellers. The pressure coefficient and the sound pressure level in the distant sound field were calculated, and the frequency filling of the spectrum of the generated sound wave was investigated. **Results and Conclusions.** Numerical calculations of the problem of aerotaxi rotation noise generation showed that the maximum pressure level in the generated waves is in the immediate vicinity of the location of the quadrotor screws. However, the maximum value of the pressure level depends on the parameters of the problem, which vary: the thickness of the blade and the speed of the horizontal flight of the aerotaxi. As one moves away from the screws, the local maxima disappear and the wave takes the form of a flat wave. The general level of generated sound (rotational noise) is in the range of 70dB-102dB, which coincides with the results of studies of quadrotor aerotaxi, as well as taxis with the arrangement of propellers according to the aircraft type. The generated rotational noise energy is concentrated in the first 4-5 harmonics. Therefore, the noise model of aerodynamic origin proposed in this study can be used to study the rotation noise of a quadrotor type aerotaxi.

Keywords: generation of aerotaxi rotation sound; calculation of sound field characteristics.

Introduction

The need for mobile movement of small groups of people within a few hundred kilometers naturally led to the search for aircraft designs that can solve this problem. One of the solutions is a quadrotor (4 propellers) air taxi, Fig. 1. Today, there are also air taxis equipped with 6 and 8 propellers. Based on the size of existing air taxi models, such constructions can be classified as small aircraft. Structurally, air taxis are built like vertical take-off aircraft. The lift is generated by screws rotating in a horizontal plane. Air taxis differ

from helicopters of the classical single-rotor design by the presence of several (4, 6, 8) symmetrically arranged propellers. The placement of the propellers, the adjustment of the blade angle to the flow, and the ability to rotate the propellers at different speeds allow the air taxi to move in the horizontal plane, performing the necessary maneuvers.

The air taxi is a relatively new type of transport, and more and more attention is being paid to its research and development. One of the problems of improving air taxis is reducing the level of aerodynamic noise. This problem is typical for helicopters and is also present in

air taxis. Acoustic noise is a source of environmental pollution that negatively affects the human psyche. A number of scientists around the world are looking for ways to reduce it. Below is a brief overview of the current research on noise from quadcopters and quadrotor air taxis.



Fig.1 Air taxi a quadrotor type

The existing works can be divided into three areas of research:

- 1) studying the flow around the quadrotor blades;
- 2) modeling the noise of aerodynamic origin of the blade-flow interaction; 3) the impact of acoustic noise on the human psyche.

The rotational noise that is the subject of this paper was first modelled by Gutin [1] for an aircraft propeller. However, this model is very simplified, taking into account only the load distribution along the blade span. The Ffowcs-Williams-Hawkings equation [2] is based on Lighthill's acoustic analogy, which has many questions, i.e. it is far from perfect. The Farassat [3] model is based on the idea of introducing artificial, non-existent sound sources inside a rigid blade. This model actually describes the process of sound generation by sources that do not exist in reality. Therefore, knowing the shortcomings of modelling the sound generation process, the author of this paper proposed an improved sound generation model [4], which allows studying the aerodynamic noise from the interaction of the blade with the air flow.

One of the important issues in modeling the noise of quadrotors is the choice of an appropriate flow model around the rotor blade and fuselage of the quadrotor. In [5], a nonlinear method of vortices in the lattice is used to calculate the loads on the blades. The calculated data are used to calculate the far sound field. Papers [6, 7] use a CFD model of increased accuracy. The accuracy of the calculation is achieved by using different numerical methods for solving the problem computational grids, for different flow regions around the blades of rotating propellers. Acoustic noise was calculated based on the Farassat model.

In [8, 9] blade element theory is used as a model of the flow around the blade. In these papers, the tonal and broadband noise for different air taxi flight conditions is studied. However, the blade element model used is very simplistic, as it does not take into account compressibility and viscosity effects.

Paper [10] presents a method for calculating the aerodynamic characteristics of a rotor propeller based on a combination of the discrete vortex method and the plane section method. A brief overview of the main nonlinear aerodynamic models used to calculate flow characteristics is given in [11]. In particular, these are the Reynolds-averaged Navier-Stokes equations (RANS, URANS) and the method of large eddy simulation (LES). However, these approaches are rather simplified from the acoustic point of view: averaging and not taking into account small changes in the flow lead to an inaccurate physical model of sound generation.

For example, in [12], different types of noise were calculated: displacement noise, isolated rotor load noise, and quadrotor noise. To model the noise, the acoustic analogy, the Ffowcs-Williams-Hawkings equation in the formulation of Farassat 1A, is used. It was assumed that monopole and dipole sound sources were distributed on the blade surface. The directivity diagrams for an isolated rotor and for the quadrotor as a whole [12] indicate that the noise of the quadrotor is significantly higher than that of a single rotor. An integral approach using the variational principle was used in [13].

The calculation was performed for a quadcopter with a rotor radius of 6cm and a rotation frequency of 17387RPM-20133RPM. The maximum noise level was achieved at a frequency of 600-700Hz and was about 85 dB – 97 dB. Similar studies were performed in [14]. The radius of the quadrotor rotor was 12 cm, the length of the blade chord was 2.5 cm, and the test rotation range was 2500RPM-8000RPM. The acoustic pressure was calculated for different positions of the observer. The peak noise level was about 74 dB. The acoustic noise of the quadrotor at low heights was experimentally studied in [15]. In particular, depending on the flight mode (start, hover mode, flight at marching speed, and landing), the maximum sound pressure level was observed at frequencies of 400 Hz – 600 Hz, and the noise spectrum showed the predominance of the first 3-4 harmonics at frequencies from 100 Hz to 800 Hz. In [16], the rotational noise of a quadrotor is modeled taking into account the Gutin model. An experimental study of the spectrum of mixed electromagnetic and acoustic noise under conditions of horizontal flight and various maneuvers, flying altitudes, taking into account reflection, and interference from the objects present is presented in [17]. The dominance of noise components in different modes of

quadrocopter operation was revealed. It was found that the noise spectrum of the quadrocopter changes with height. This is due to the variable properties of the atmosphere, in particular, the presence of turbulent phenomena. The issues of detecting quadrocopters in urban interference are discussed in [18]. Since the noise of quadrocopters differs from that of helicopters, the noise level and its spectrum differ from that of helicopters. This issue is also discussed in [18].

Recently, more and more attention has been paid to assessing the impact of quadcopter noise radiation on the human psyche. This paper [19] first describes the main acoustic and operational characteristics of drones, as an unconventional noise source compared to conventional civil aircraft. In paper [20] notes that drone noise is specific and more annoying than road noise and aircraft noise. The impact of noise from different types of drones (quadrotors, hexavectors) on humans was studied in [21]. In particular, it was found that hexavectors have a more negative impact than quadrotors. The impact of various sources of drone-generated noise was assessed using microphones and numerical modulation in [22]. The effect of noise on humans from four different types quadrocopters and the assessment of the psychoacoustic effect was studied [23]. This area of research is actually a continuation of the study of the impact of helicopter noise on the environment.

Almost all of the above studies are dedicated to quadrocopters, i.e. unmanned aerial vehicles. As for air taxis, there are much fewer publications on this topic. For example, paper [24] presents a CFD model of the flow around various parts of an air taxi and studies the mutual influence of the propellers and fuselage on the formation of a vortex flow. Paper [25] considers the complex problem of optimizing an air taxi flight with a number of parameters (speed, angle of attack) under certain constraints. This paper is a continuation of [7].

The results of the noise level study, when the above parameters are changed, have shown that the noise level varies from 45 dB to 120 dB depending on flight conditions and parameter optimization in different scenarios. It was found that the noise of an air taxi with 1 passenger can be completely masked by the noise of the highway at an altitude of more than 1000 feet, while the noise of an air taxi with 6 passengers can only be partially blocked by ambient noise.

Another interesting work is [26], which calculates the noise of an aircraft-type air taxi. It presents three different models: an isolated rotor configuration with 1 passenger, a full configuration with 1 passenger, and an isolated rotor configuration with 6 belt-fats. The noise comparison between the isolated rotor with 1 passenger and the full configuration shows that the vehicle fuselage can increase the sound pressure level (SPL) by

up to 5 dB. An acoustic comparison of the 1 and 6-passenger configurations shows that the maximum difference in overall sound pressure level between the two configurations is 14 dB. In addition, it is shown that the noise in the single-seat and six-seat configurations is significantly lower than that of a conventional four-blade helicopter in horizontal flight. The noise impact of aircraft on the population was assessed in comparison with the background noise of the sound field. The sound pressure level calculation data without taking into account the full layout of the air taxi ranged from 77 dB for one passenger to 92 dB for 6 passengers.

1. Problem formulation

1.1. Formulation of the aerodynamics problem

To study the rotor rotation noise of quadrotors, we use the potential flow model described by the system of equations [4]:

$$a^2 \operatorname{div}(\nabla\phi) - \nabla\phi(\nabla\phi \cdot \nabla) - 2\nabla\phi \frac{\partial \nabla\phi}{\partial t} - \frac{\partial^2 \nabla\phi}{\partial t^2} = 0 \quad (1)$$

– equations of motion in potential form.

$$\frac{\partial \phi}{\partial t} + \frac{\nabla^2 \phi}{2} + \frac{a^2}{\gamma - 1} = \frac{U^2}{2} + \frac{a_\infty^2}{\gamma - 1} \quad (2)$$

– Bernoulli's equation.

If the shape of the blade's enveloping cross-section is a function F , then the boundary condition on the blade's surface is that the fluid does not flow through the surface:

$$F_t + v\nabla F = 0. \quad (3)$$

To solve the problem of acoustics, it is necessary to distinguish small acoustic disturbances of the flow. For this purpose, we introduce dimensionless coordinates.

1.2. Dimensionless coordinate system, formulation of the acoustics problem

We assume that the blades of the quadrotor screws are subjected to a flow with a velocity U , which generates small acoustic disturbances ϕ' in the process of interaction with the blades. Based on the above, the flow potential can be represented as follows:

$$\phi = U(x + \phi'). \quad (4)$$

Let's enter the dimensionless coordinates:

$$\xi = \frac{x}{c}, \eta = \lambda y, \zeta = \frac{z}{R}, \tau = kt. \quad (5)$$

The equation describing the generation and propagation of small sound vibrations is written in the form [4]:

$$\left(\frac{kc}{U}\right)^2 f_{\tau\tau} + \left[1 - \frac{1}{M_1^2} + (1 + \gamma)\varepsilon f_\xi\right] f_{\xi\xi} + 2\frac{kc}{U} f_{\xi\tau} - \frac{(\lambda c)^2}{M_1^2} f_{\eta\eta} - \left(\frac{c}{R}\right)^2 \frac{1}{M_1^2} f_{\zeta\zeta} = 0, \quad (6)$$

where $f(\xi, \eta, \zeta, \tau)$ is the potential of small acoustic interactions associated with small perturbations of the full flow potential by expression:

$$\varepsilon \cdot f(\xi, \eta, \zeta, \tau) = \frac{\phi'}{c}. \quad (7)$$

After simplifications, boundary condition (3) will take the form:

$$-f_\eta + \varepsilon f_\xi g_\xi = -g_\xi. \quad (8)$$

Equations (6) with boundary condition (8) constitute the boundary value problem for the sound potential $f(\xi, \eta, \zeta, \tau)$. It should be noted that the boundary condition (8) is set on the inner part of the boundary of the computational domain of the sound potential. On the outer boundary of the domain, a sphere of large radius, the Sommerfeld radiation conditions are set. They are taken into account in the integral expression for the far field presented later in this paper. Since the potential is a function of time, it is necessary to specify additional initial conditions. Before the interaction with the blade, the flow was undisturbed, i.e., the potential and its time derivative are zero:

$$f|_{\tau=0} = f_\tau|_{\tau=0} = 0. \quad (9)$$

2. Method of solving the problem

It should be noted that the equation for the propagation of small disturbances (6), depending on the domain of realization of the flow parameters, can be of either elliptic or hyperbolic type. Therefore, standard finite-difference schemes do not allow solving such problems numerically. The numerical-analytical method developed by the author [27, 28] allows for solving such problems.

The numerical-analytical method was tested on the problems of sound generation by a helicopter blade for subsonic flow [29], studying the effect of blade curva-

ture and shape on rotational noise [30], studying the noise of a helicopter rotor when the helicopter blade is obliquely blown [31], and the effect of variation in the cross-sectional shape along the blade span on rotational noise [32]. In the non-stationary three-dimensional problem, the 15-point scheme of the method was used.

3. Analysis of the sound near-field calculation data

As a test configuration, a radius $R = 3 \text{ m}$ blade with a chord $c = 0.3 \text{ m}$ was used in the air taxi. In cross-section, the blade has a NASA parabolic profile. As a result of the numerical solution of the above boundary value problem, we have numerical values of the potential and its derivatives. Since the cross-section of the blade is a thin wing profile, the behavior in the pressure wave of the near-sound field can be studied using the pressure coefficient:

$$C_p = 2\varepsilon \cdot (k \cdot f_\tau + f_\xi + \frac{1}{2}\varepsilon \cdot \lambda^2 \cdot f_\eta^2). \quad (10)$$

The pressure coefficient shows how the pressure over the blade changes as the blade flows around the flow. Since the pressure coefficient is a function of the sound potential f , it reflects the intensity of sound generation in different parts of the blade surface.

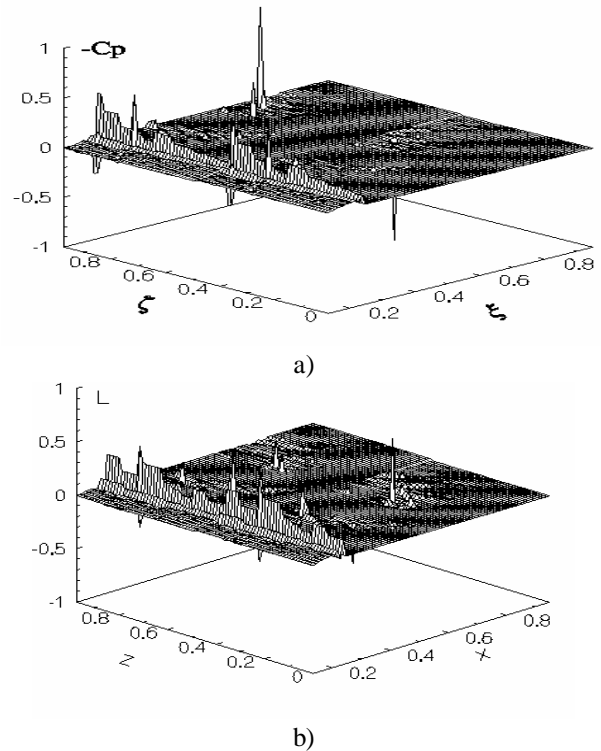


Fig. 2. The pressure coefficient:
a) $M = 0.1$; b) $M = 0.2$

Let us analyze the pressure coefficient calculations made for two different specific blade thicknesses $\delta=0.06; 0.1$ and two different values of the Mach number $M=0.1; 0.2$ corresponding to the actual horizontal flight speeds of an air taxi. It was assumed that the rotational speed of each propeller is $\Omega R = 220\text{m/s}$.

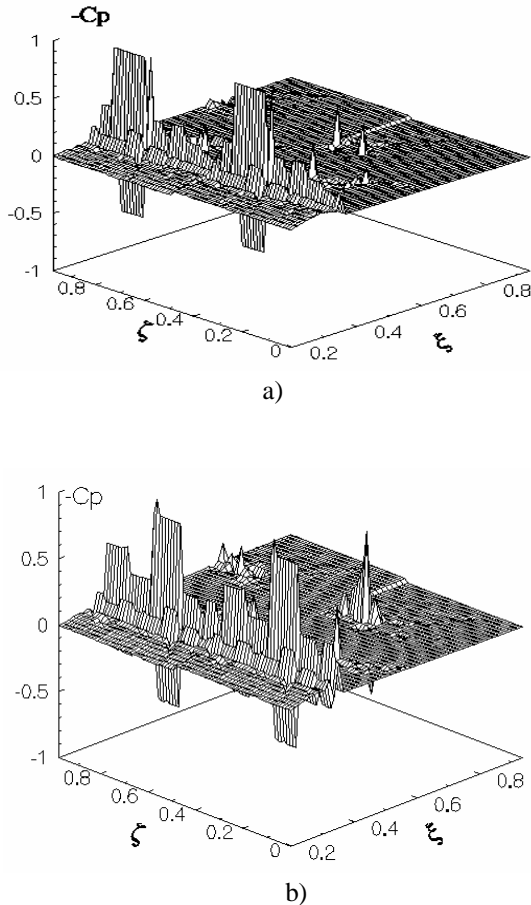


Fig. 3. The pressure coefficient:
a) $M = 0.1$; b) $M = 0.2$

The curves C_p in Fig. 2 ($\delta=0.06$) and Fig. 3 ($\delta=0.1$) show that the thickness blade disturbs the flow much less than the thickness blade. The maximum level and nature of the main series of peaks at $\xi=0.36$ depend on the Mach number. Thus, for Mach number $M=0.2$, the peaks C_p have larger amplitudes and are more densely distributed along the blade span than in the case of $M=0.1$. In addition to the main series of perturbations realized along the blade swing, additional zones of sound generation appeared in two places at $\xi=0.7$. At the same time, they are more pronounced for Mach number $M=0.2$ than for Mach number $M=0.1$.

4. Far sound field

The integral representation using the second Green's formula is generally accepted as a model of the far sound field. It allows, knowing the distribution of acoustic sources on the blade surface, to describe the sound field at each point of its existence at different distances from the area of direct sound generation. When deriving a representation of the far sound field, boundary conditions on a sphere of large radius, at a considerable distance from the blade surface, are taken into account. These conditions are the Sommerfeld radiation conditions [33]. Their essence is that with a significant increase in the radius of the sphere at infinity, the sound potential and its first derivatives tend to be zero. At the same time, the total sound energy remains constant if there is no attenuation in the medium.

The distinctive feature of each such representation is only the equation, taking into account which this integral representation is obtained. If we are talking about the three-dimensional nonstationary propagation of small sound disturbances from a thin body, a rotor blade, then this representation is given in [4]:

$$\begin{aligned}
 4\pi\phi' = & -M_1^2 \int_S \left[\frac{1}{R} (\phi'_x + \frac{1}{2}(1+\gamma)(\phi'_x)^2) \right]_{t^*} dS_x - \\
 & - \frac{2M_1^2}{U} \int_S \left[\frac{\phi'_t}{R} \right]_{t^*} dS_x + \\
 & + \int_S \left[\frac{1}{R} \frac{\partial \phi'}{\partial n} + \frac{1}{Ra_\infty} \frac{\partial R}{\partial n} \frac{\partial \phi'}{\partial t} - \phi' \frac{\partial}{\partial n} \left(\frac{1}{R} \right) \right]_{t^*} dS
 \end{aligned} \quad (10)$$

In work [4], representation (10) was used to numerically calculate the sound field of rotating propellers (rotational noise). The peculiarity of this problem is that the total far sound field is formed taking into account the sound generation by each of the 4 air taxi propellers, Fig. 4.

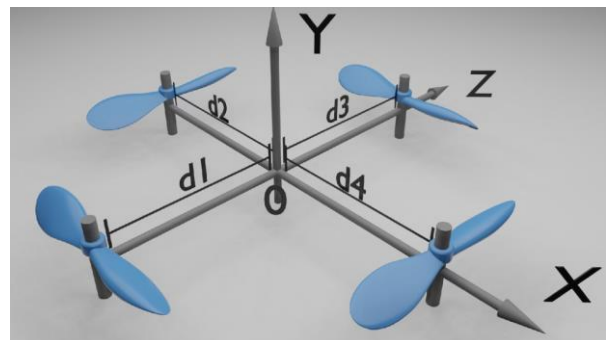


Fig. 4 Scheme of air taxi screws placement

Therefore, the sound potential ϕ' is a superposition of the sound potential of 4 rotors:

$$\phi' = \phi'_1 + \phi'_2 + \phi'_3 + \phi'_4, \quad (11)$$

where

$$4\pi\phi'_i = -M_1^2 \int_{S_i} \left[\frac{1}{R} (\phi'_{ix} + \frac{1}{2}(1+\gamma)(\phi'_{ix})^2) \right]_{t^*} dS_{ix} - \frac{2M_1^2}{U} \int_{S_i} \left[\frac{\phi'_{it}}{R} \right]_{t^*} dS_{ix} + \int_{S_i} \left[\frac{1}{R} \frac{\partial \phi'_i}{\partial n} + \frac{1}{Ra_\infty} \frac{\partial R}{\partial n} \frac{\partial \phi'_i}{\partial t} - \phi'_i \frac{\partial}{\partial n} \left(\frac{1}{R} \right) \right]_{t^*} dS_i \quad (12)$$

In equation (12), the index values $i=1, \dots, 4$ correspond to the four surfaces S_i of the air taxi rotors. The far field is presented in dimensional values. This is necessary in order to perform a comparative analysis of the values obtained as a result of the calculation with the available experimental data. A square of size $[x \times z] = [-4\text{m}; 4\text{m}] \times [-4\text{m}; 4\text{m}]$, which covers the entire area of the air taxi propellers, was selected as the calculated area for recording the generated sound (noise) level. This allows us to see the general picture of the formation of the sound field over the air taxi as a whole.

Fig. 5 and Fig. 6 show the distribution of the sound pressure level for the case $\delta = 0.06; M = 0.1$. It should be noted that there are 4 local areas of increased sound generation in the specified computational square. These areas correspond to the locations of 4 air taxi rotors. However, the mutual influence of the sound fields of each of the air taxi rotors is such that the pressure concentration in the area of individual rotors is slightly higher than that of other rotors. The sound pressure level is in the range of 70dB-85dB. The sound pressure level decreases with increasing distance from the calculated area.

With an increase in the Mach number $M = 0.2$, Fig. 7, the pressure level increased by 3dB compared to the case of $M = 0.1$. This indicates the direct influence of the flow velocity flowing around the blade on the intensity of sound generation and its level.

Increasing the relative blade thickness to the value of $\delta = 0.1$, Fig. 8-11, resulted in a significant increase in the generated noise level to 95 dB. At the same time, the pattern of distribution of the peaks in the sound wave changed slightly: the peaks became more pronounced. With increasing distance from the control surface, the local areas of the maximum pressure level significantly

decrease, levelling out with the overall sound pressure level. Thus, at a distance of $y = 5.0$ m, Fig. 9, b, the sound wave has a shape close to a plane sound wave.

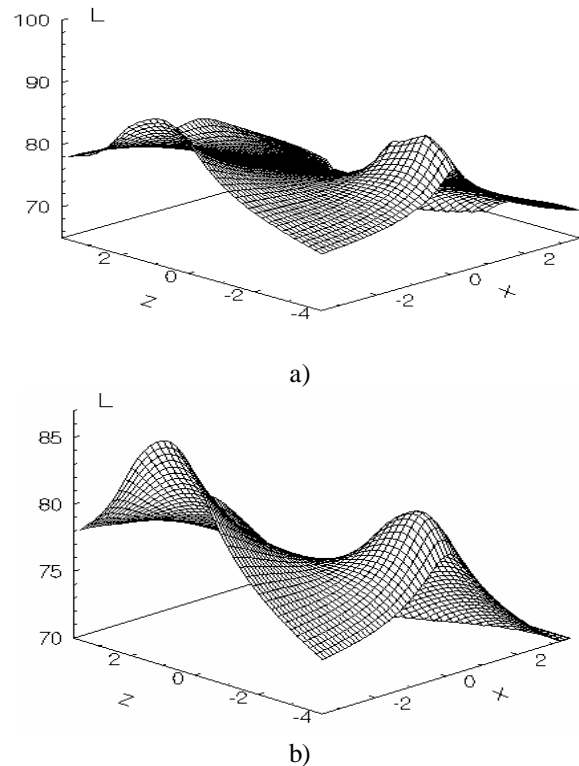


Fig. 5. Sound pressure level, dB:
a) $y=0.2$ m, b) $y=0.5$ m

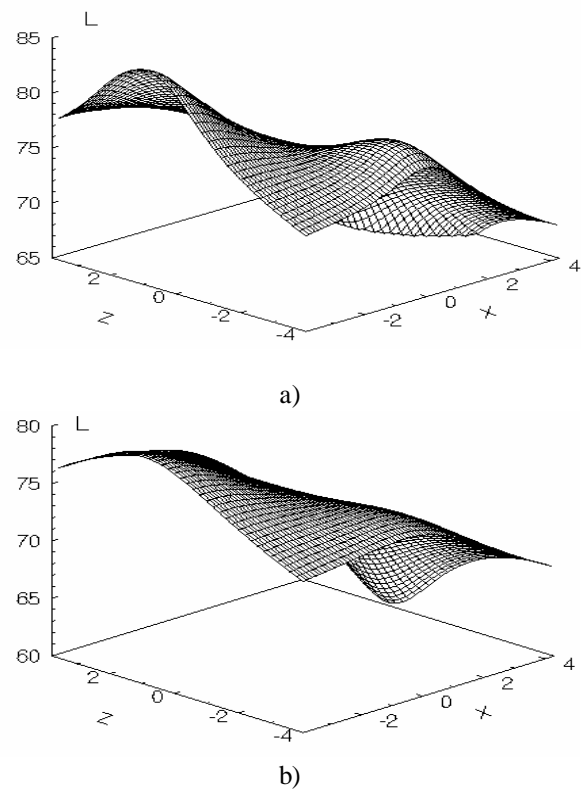
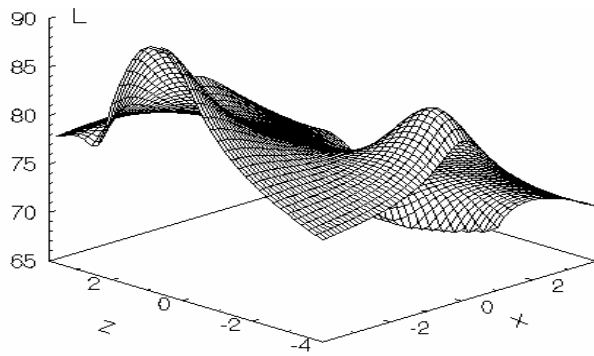
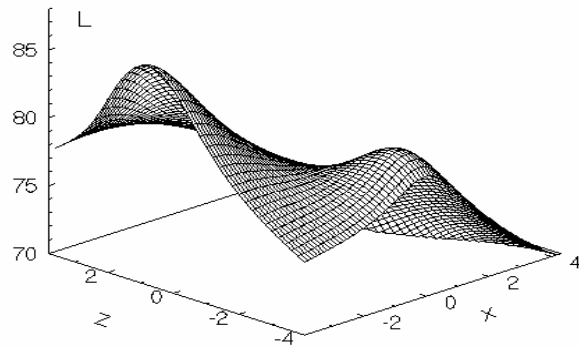


Fig. 6. Sound pressure level, dB:
a) $y=1.0$ m, b) $y=2.0$ m

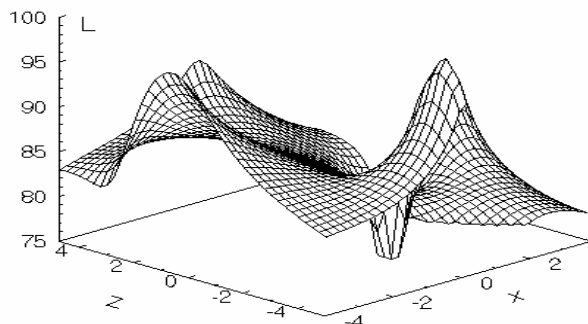


a)

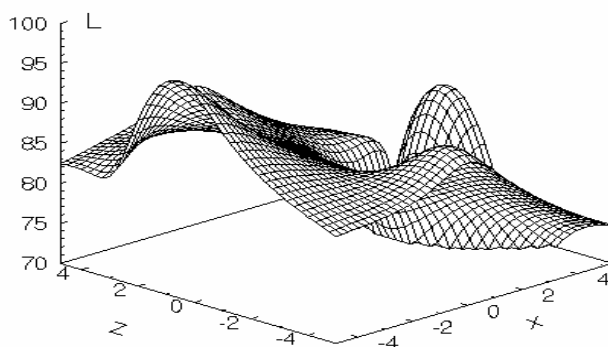


b)

Fig. 7. Sound pressure level, dB:
a) $y=0.5$ m, b) $y=1.0$ m

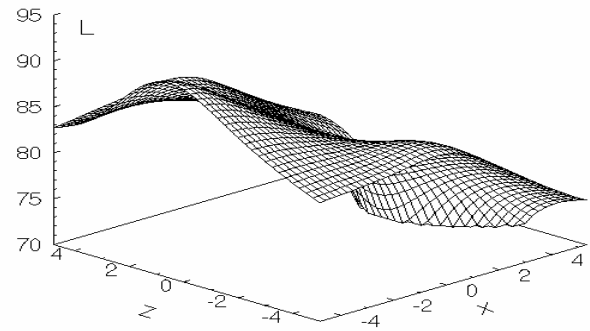


a)

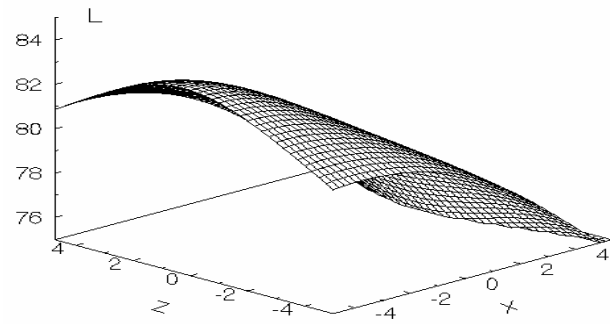


b)

Fig. 8. Sound pressure level, dB:
a) $y=0.2$ m, b) $y=1.0$ m



a)



b)

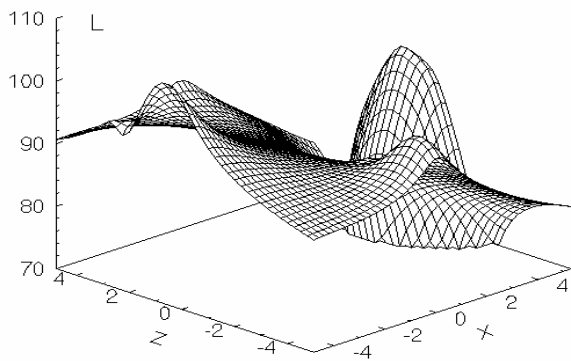
Fig. 9. Sound pressure level, dB:
a) $y=2.0$ m, b) $y=5.0$ m

Increasing the Mach number to $M=0.2$, Fig. 10 and Fig. 11, resulted in a significant local variation of the sound pressure level in the area of one of the screws. This indicates that there is a significant non-stationarity in the flow, which leads to sharp changes in the sound pressure level. At the same time, the total sound pressure level increased to 105 dB. With an increase in distance from the calculation area, these peaks are smoothed out, but the total sound pressure level is 3 dB higher than in the case of $M=0.1$.

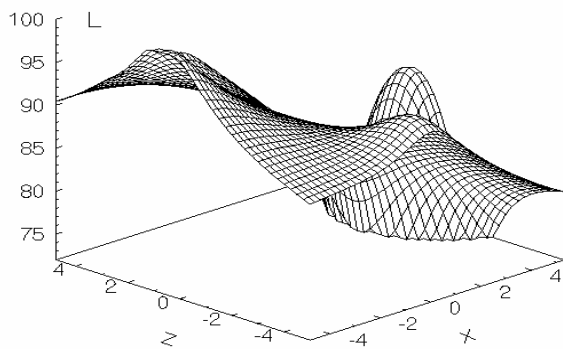
Paper [26] presents data on the sound field level from the operation of 4 propellers arranged in a single row for an aircraft-type air taxi. There are 2 propellers on each of the wings of the airframe. As mentioned in the introduction, the noise from the propellers of this air taxi ranges from 77 dB to 92 dB. The noise calculations of the quadrotor type air taxi studied above fall within the same noise range. Thus, the model used in this study to calculate the noise of the aerodynamic origin of a quadrotor-type air taxi is quantitatively consistent with the available calculated data of close analogs of air taxis.

Another important characteristic of the generated sound is the spectral content of harmonics. As can be seen from Fig. 12, the main energy in the radiation spectrum is concentrated in the first 7-8 harmonics for the case of $\delta=0.06; M=0.1$. The activation of the harmonic near 400 Hz is also noticeable (light ridge in Fig. 12, a). With increasing Mach number $M=0.2$ and

blade thickness $\delta = 0.1$, the sound energy is concentrated in the first 4-5 harmonics.

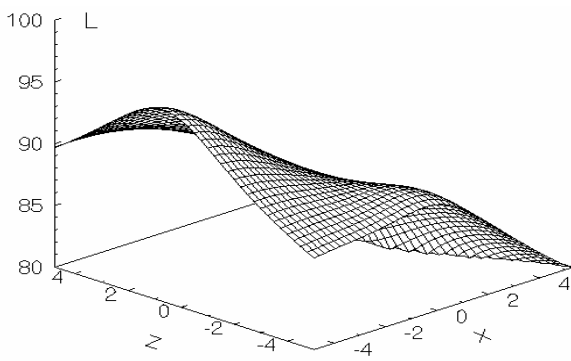


a)

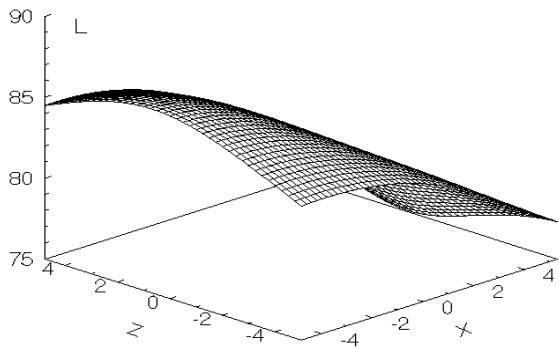


b)

Fig. 10. Sound pressure level, dB:
a) $y=0.5$ m, b) $y=1.0$ m

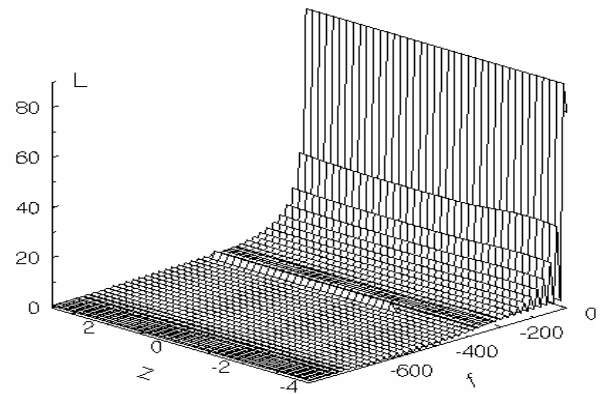


a)

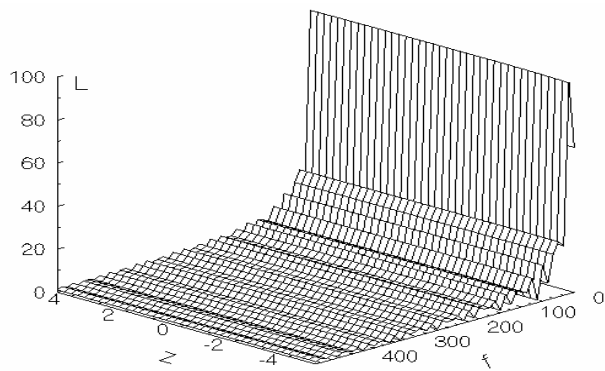


b)

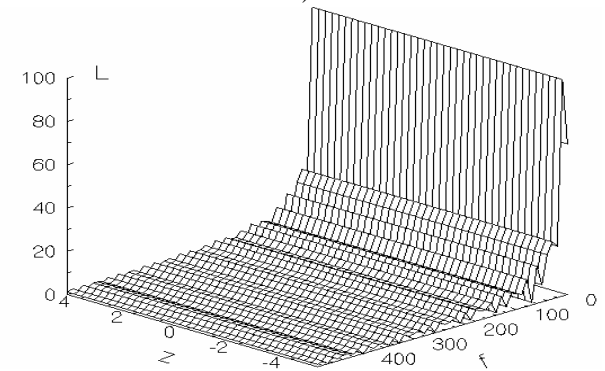
Fig. 11. Sound pressure level, dB:
a) $y=2.0$ m, b) $y=5.0$ m



a)



b)



c)

Fig. 12. Frequency spectrum of a sound wave:
a) $\delta = 0.06; M = 0.1$, b) $\delta = 0.1; M = 0.1$,
c) $\delta = 0.1; M = 0.2$

Discussion

The problem solved above is one of the possible variants of modeling the rotational noise of the aerodynamic origin of a quadrotor-type air taxi. The three-dimensional unsteady flow model used in the potential approximation has certain limitations. However, these limitations relate to the vortex noise, not to the rotational noise, which is described quite accurately in the potential approximation. Nevertheless, the existing Gutin and Fowkes-Williams-Hawkings models are not accurate compared to the model used in this paper, since they do not physically correctly extract

sound from unsteady flow. The solved problem does not take into account the secondary wave reflected from the air taxi fuselage. However, this will not affect the maximum sound pressure level, since the reflected wave is already significantly attenuated. This issue can be taken into account in a further study when a model using the secondary flow around the air taxi blade is applied.

Conclusions

The paper analyses the studies on modelling the flow around the blades of quadrotors and the methods for calculating the acoustic field generated by the aerodynamic interaction of the flow and the blades.

The problem of generating rotational noise by the blades of a quadrotor-type air taxi is formulated and numerically solved in the potential approximation. The characteristics of the near and far sound fields are studied. In particular, the pressure coefficient and the sound pressure level in the far sound field are calculated, and the frequency content of the generated sound wave spectrum is investigated.

The total level of generated rotational noise is in the range of 70dB-102dB, which is quite close to the results of studies of a quadrotor air taxi, and is also close to an air taxi with an aircraft-type propeller arrangement. The energy of the generated rotational noise is concentrated in the first 4-5 harmonics. Thus, the noise model of aerodynamic origin proposed in this paper can be used to study the rotational noise of quadrotor-type air taxis.

In further research, it is planned to study the noise of air taxis generated during various malfunctions.

Contribution of authors: conceptualization – **Petro Lukianov, Oleg Dusheba**; formulation of task – **Petro Lukianov**; analysis – **Petro Lukianov, Oleg Dusheba**; software – **Oleg Dusheba**; development of mathematical model – **Petro Lukianov**; analysis of results – **Petro Lukianov, Oleg Dusheba**.

All the authors have read and agreed to the published version of the manuscript.

References

1. Gutin, L. Ya. *On the sound field of a rotating propeller. National Advisory Committee For Aeronautics. Technical Memorandum No. 1195*, NACA, Washington, October, 1948. 22 p. Available at: <https://ntrs.nasa.gov/api/citations/20030068996/downloads/20030068996.pdf>. (accessed Jan. 12, 2023).

2. Ffowcs Williams, J. E. & Hawkins, D. L. *Theory Relating to the Noise of Rotating Machinery.*

Journal of Sound and Vibration, 1969, vol. 10, no. 1, pp. 10-21. DOI: 10.1016/0022-460X(69)90125-4.

3. Farassat, F. Derivation of Formulations 1 and 1A of Farassat. *NASA/TM-2007-214853*. – NASA Langley Research Center, Hampton, Virginia, March, 2007. Available at: <https://ntrs.nasa.gov/api/citations/20070010579/downloads/20070010579.pdf>. (accessed Jan. 12, 2023).

4. Lukianov, P. V. Nestacionarnoe rasprostranenie malyh vozmushhenij ot tonkogo kryla: blizhnee i dal'nee pole [Unsteady propagation of small disturbances from a thin wing: The near and far field]. *Akustichnyj visnyk – Acoustic bulletin*, 2009, vol. 12, no. 3, pp. 41-55. Available at: <http://dspace.nbuv.gov.ua/handle/123456789/87285>. (accessed Jan. 12, 2023).

5. Lee, H. & Lee, D.-J. Rotor interactional effects on aerodynamic and noise characteristics of a small multirotor unmanned aerial vehicle. *Phys. Fluids*, 2020, vol. 32, iss. 4, article no. 047107, pp. 1-18. DOI: 10.1063/5.0003992.

6. Jia, Z., Lee, S., Sharma, K. & Brentner, K. S. Aeroacoustic analysis of a liftoff coaxial rotor using high-fidelity CFD/CSD loose coupling simulation. *J. Am. Helicopter Soc.*, 2020, vol. 65, iss. 1, pp. 1-15. DOI: 10.4050/JAHS.65.012011.

7. Jia, Z. & Lee, S. Computational Study on Noise of Urban Air Mobility Quadrotor Aircraft. *J. Am. Helicopter Soc.*, 2022, vol. 67, iss. 1, pp. 1-15. DOI: 10.4050/JAHS.67.012009.

8. Kevin Li, S. & Lee, S. Prediction of Urban Air Mobility Multirotor VTOL Broadband Noise Using UCD-QuietFly. *J. Am. Helicopter Soc.*, 2021, vol. 66, iss. 3, pp. 1-13. DOI: 10.4050/JAHS.66.032004.

9. Kevin Li, S. & Lee, S. Acoustic Analysis and Sound Quality Assessment of a Quiet Helicopter for Air Taxi Operations. *J. Am. Helicopter Soc.*, 2021, vol. 67, iss. 3, pp. 1-15. DOI: 10.4050/JAHS.67.032001.

10. Lebed, V. G., Kalkamanov, S. A. & Pchelnikov, S. I. Metod rascheta aerodinamicheskikh kharakteristik rotornogo vinta [The method of calculation of aerodynamic characteristics rotary screw]. *Aviacijno-kosmicna tehnika i tehnologia – Aerospace technic and technology*, 2016, vol. 5, pp. 29-34. Available at: http://nbuv.gov.ua/UJRN/aktit_2016_5_6. (accessed Jan. 12, 2023).

11. Diachenko, O. Ju., Krivtsov, V. S. & Timchenko, O. M. Analiz metodov aerodinamicheskogo rascheta nesushchego vinta vertoletu [Analysis methods of aerodynamic calculations of helicopter's rotor]. *Aviacijno-kosmicna tehnika i tehnologia – Aerospace technic and technology*, 2014, vol. 4, pp. 22-33. Available at: http://nbuv.gov.ua/UJRN/akit_2014_4_6. (accessed Jan. 12, 2023).

12. Lee, H. & Lee, D.-J. Numerical prediction of aerodynamic noise radiated from a propeller of un-

- manned aerial vehicles. *Inter. Noise.*, 2019. June 16-19., Noise control for a better environmental, pp. 1-9. Available at: https://www.sea-acustia.es/INTERNOISE_2019/Fchrs/Proceedings/1469.pdf. (accessed Jan. 12, 2023).
13. Legendre, C., Ficat-Andrieu, V., Poulos, A., Kitano, Y., Nakashima, Y., Kobayashi, W. & Minorikawa, G. Computational noise level predictions of small multi-rotor unmanned aircraft systems at different payload condition. *DICUAM 2021-15-17* March 2021. Available at: https://www.fft.be/sites/default/files/private/dicuum_-_legendre_-_computational_noise_level_predictions.pdf. (accessed Jan. 12, 2023).
14. Thai, A. & Grace, S. Prediction of small quadrotor blade induced noise. *25th AIAA/CEAS Aeroacoustics Conference*. May 2019. 13 p. DOI: 10.2514/6.2019-2684.
15. Zaslavskii, Yu. M. & Zaslavskii, V. Yu. Akusticheskiy shum nizkoletyashchego kvadrotora [Acoustic noise of a low-flying quadrotor]. *Noise Theory and Practice*, 2019, vol. 5, iss. 5, pp. 21-27. Available at: <https://cyberleninka.ru/article/n/akusticheskiy-shum-nizkoletyashchego-kvadrokoptera/viewer>. (accessed Jan. 12, 2023).
16. Sokol, G. I., Nekrasov, V. Ye. & Zhmurko, V. S. K raschetu akusticheskogo polya vintov kvadrotora [To the calculation of the acoustic field of propellers of a quadrotor]. *Vestnik Samarskogo gosudarstvennogo tekhnicheskogo universiteta. Seriya: Fiziko - matematicheskie nauki*, 2019, vol. 27, iss. 4, pp. 42-51. Available at: https://www.researchgate.net/publication/343921265_K_RASCETU_HARAKTERISTIK_AKUSTICHESKOGO_POLA_VINTOV_KVADROKOPTERA_DO_ROZRAHUNKU_HARAKTERISTIK_AKUSTICHESKOGO_POLA_GVINTIV_KVADROKOPTERU. (accessed Jan. 12, 2023).
17. Goncharenko, B. I., Kuz'menkov, A. N. & Kotov, A. N. Eksperimental'noe issledovanie osobennosti formirovaniya spektra шумов беспилотного летательного аппарата [Experimental study of the features of the formation of the noise spectrum of an unmanned aerial vehicle]. *Noise theory and practice*, 2021, vol. 6, iss. 4, pp. 49-59.
18. Sokolov, G. E. Analiz akusticheskikh informatsionnykh signalov kvadrokopteroiv i pomekhovykh zvukov goroda [Analysis of acoustic information signals of quadcopters and interference sounds of the city]. *Problemy informatyzacii' ta upravlinnja*, 2021, vol. 67(3), pp. 61-70. Available at: <https://jrn1.nau.edu.ua/index.php/PIU/article/view/16208/23458>. (accessed Jan. 12, 2023).
19. Torija, A. J. & Clark C. A Psychoacoustic Approach to Building Knowledge about Human Response to Noise of Unmanned Aerial Vehicles. *International Journal of Environmental Research and Public Health*, 2021, vol. 18, iss. 2, article no. 682. DOI: 10.3390/ijerph18020682.
20. Schäffer, B., Pieren, R., Heutschi, K., Wunderli, J. M. & Becker, S. Drone Noise Emission Characteristics and Noise Effects on Humans – A Systematic Review. *Int. J. Environ. Res. Public Health*, 2021, vol. 18, iss. 11, article no. 5940. DOI: 10.3390/ijerph18115940.
21. Ivošević, J., Ganić, E., Petošić, A. & Radišić, T. Comparative UAV Noise-Impact Assessments through Survey and Noise Measurements. *Int. J. Environ. Res. Public Health*. 2021, vol. 18, iss. 12, article no. 6202. DOI: 10.3390/ijerph18126202.
22. Yamada, T., Itoyama, K., Nishida, K. & Nakadai, K. Assessment of Sound Source Tracking Using Multiple Drones Equipped with Multiple Microphone Arrays. *Int. J. Environ. Res. Public Health.*, 2021, vol. 18, iss. 17, article no. 9039. DOI: 10.3390/ijerph18179039.
23. Hui, C. T. J. , Kingan, M. J., Hioka, Y., Schmid, E., Dodd, G., Dirks, K. N., Edlin, S., Mascarenhas, S. & Shim, Y.-M. Quantification of the Psychoacoustic Effect of Noise from Small Unmanned Aerial Vehicles. *Int. J. Environ. Res. Public Health.*, 2021, vol. 18, iss. 17, article no. 8893. DOI: 10.3390/ijerph18178893.
24. Diaz, P. V. & Yoon, S. Computational Study of NASA's Quadrotor Urban Air Taxi Concept. *AIAA SciTech Forum.*, 6-10 January 2020, Orlando, FL. DOI: 10.2514/6.2020-0302.
25. Sagaga, J. & Lee, S. Acoustic Predictions for the Side-by-Side Air Taxi Rotor in Hover. *Vertical Flight Society Forum 77*, May 2021. DOI: 10.4050/F-0077-2021-16695.
26. Orndorff, N. C., Scotzniovsky, L. & Sarojini, D. Air-taxi transition trajectory optimization with physics-based models. *AIAA SCITECH 2023 Forum*. Jan 23-27, 2023, National Harbor, MD. DOI: 10.2514/6.2023-0324.
27. Lukianov, P. V. Primenenie chislennanaliticheskogo metoda dlja reshenija zadach akustiki [Application of the numerical-analytical method for solving problems of acoustics]. *Akustychnyj simpozium «Konsonans-2005»*, Kyiv, 27-29 veresnja 2005, pp. 225-230. Available at: http://hydromech.org.ua/content/pdf/cons/cons2005_225-230.pdf. (accessed Jan. 12, 2023).
28. Lukianov, P. V. Ob odnom chislennanaliticheskom podhode k resheniju zadachi generacii zvuka tonkim krylom. Chast' II. Shema prilozhenija k nestacionarnym zadacham [On one numerical-analytical approach to solving of a problem on sound generation by a thin wing. Part II. A schematic of application to non-stationary problems]. *Akustychnyj visnyk – Acoustic bulletin*, 2012, vol. 15, iss. 3, pp. 45-52. Available at:

http://hydromech.org.ua/content/ru/av/15-3_45-52.html. (accessed Jan. 12, 2023).

29. Lukianov, P. V. Generatsiya zvuku pri dozvukovomu obtikanni gvinta gelikoptera [Sound Generation by Helicopter Blade Swept by Subsonic Flux]. *Naukovi visti Natsional'nogo tekhnichnogo universitetu Ukraini "Kiivs'kii politekhnichnii institut" - Research Bulletin of National Technical University of Ukraine "Kyiv Polytechnic Institute"*, 2011, no. 4, pp. 143-148. Available at: <https://ela.kpi.ua/handle/123456789/36757>. (accessed Jan. 12, 2023).

30. Lukianov, P. V. Vpliv formi, krivizni poperechnogo pererizu lopati rotra gelikoptera na parametri shumu obertanyaya [Blade Shape and Cross Section's Curvature Influence Parameters of the Rotor's Rotational Noise]. *Naukovi visti Natsional'nogo tekhnichnogo universitetu Ukraini "Kiivs'kii politekhnichnii institut" - Research Bulletin of National Technical University of Ukraine "Kyiv Polytechnic Institute"*, 2012, no. 4, pp. 149-153. Available at:

<https://ela.kpi.ua/handle/123456789/36878>. (accessed Jan. 12, 2023).

31. Lukianov, P. V. Generatsiya zvuka lopatty gelikoptera pri kosomu obduvanni potokom [Sound generation by helicopter's blade at oblique angle of flow blow]. *Visnik Kiivs'kogo natsional'nogo universitetu imeni Tarasa Shevchenka. Seriya: fiziko-matematichni nauki - Bulletin of Taras Shevchenko National University of Kyiv Series: Physics & Mathematics*, 2011, no. 4, pp. 91-94. Available at: <https://bphm.knu.ua/index.php/bphm/issue/view/30>. (accessed Jan. 12, 2023).

32. Lukianov, P. V. Variatsiya formy prodol'nogo secheniya lopasti vertoleta pri modelirovanii shuma vrashcheniya [Shape variation of the helicopter's blade longitudinal section for rotational noise simulation]. *Visnyk Cherkas'kogo universytetu. Seriya: Prykladna matematyka. Informatyka*, 2012, no. 18(231), pp. 15-22.

33. Lependin, L. F. *Akustika* [Acoustics]. Moscow, "Vysshaja shkola" Publ., 1978. 448 p.

Надійшла до редакції 11.06.2023, розглянута на редколегії 08.08.2023

МОДЕЛЮВАННЯ АЕРОДИНАМІЧНОГО ШУМУ АЕРОТАКСІ КВАДРОТОРНОГО ТИПУ

Петро Лук'янов, Олег Душеба

Предметом даної роботи є дослідження сучасного стану моделювання течії навколо лопатей квадрокоптерів, моделей генерації звуку аеродинамічного походження, постановка та чисельне розв'язання задачі генерації шуму обертання лопатями аеротаксі квадаторного типу. До моделей, що описують поле течії навколо лопатей квадаторів слід віднести моделі нелінійних вихорів у ґратах, осередненого за Рейнольдцем рівняння Нав'є-Стокса (RANS, URANS), метод моделювання великих вихорів (LES), а також пряме чисельне моделювання (DNS) системи рівнянь аеродинаміки. В роботі виконано аналіз основних моделей шуму аеродинамічного походження різного типу. Для опису шуму обертання квадатора користуються моделлю Гутіна, а для моделювання шуму з урахуванням різних звукових джерел використовують рівняння Фоукс-Уільямса-Хоукінґса у формулюванні Фарассата. Однак ці підходи мають певні недоліки, що обмежують зазначені моделі у застосуванні. У наведеній нижче роботі використано сучасний підхід моделювання шуму аеродинамічного походження на основі 3-х вимірною нестационарного рівняння поширення звуку від тонкої лопаті в потенційному наближенні. Використовуючи даний підхід, виконано чисельний розрахунок задачі генерації звуку (шуму обертання) аеродинамічного походження аеротаксі квадаторного типу. **Мета дослідження.** Незважаючи на описані вище підходи, існує проблема, пов'язана з досягненням прийнятної рівня шуму, тобто його подальшим зниженням. Для вирішення цієї проблеми існує необхідність використання більш точних моделей, які дозволять проводити дослідження щодо зменшення шуму аеротаксі. **Задачі дослідження.** У зв'язку з цим була поставлена і вирішена задача моделювання шуму аеродинамічного походження з використанням уточненої моделі звуку, що генерується при взаємодії потоку і лопатей повітряного таксі. **Методи дослідження засновані на** побудові та використанні математичної моделі генерації звуку обертання, що генерується спільною роботою роторів аеротаксі. На її основі виконано розрахунок ближнього та дальнього звукових полів. Запропоновано нову модель розрахунку звукового дальнього поля аеротаксі квадаторного типу, що враховує взаємне формування результуючого звукового поля від спільної роботи 4-х гвинтів. Виконано розрахунок коефіцієнта тиску, рівня звукового тиску в дальньому звуковому полі, досліджено частотне наповнення спектра звукової хвилі, що генерується. **Результати та висновки.** Числові розрахунки задачі генерації шуму обертання аеротаксі показали, що максимуми рівня тиску в хвилі, що генерується, знаходяться в безпосередній близькості від розташування гвинтів квадатора. Однак значення максимумів рівня тиску залежить від параметрів задачі, що варіюються: товщини лопаті і швидкості

горизонтального польоту аеротаксі. У міру віддалення від гвинтів локальні максимуми зникають і хвиля набуває форми плоскої хвилі. Загальний рівень генерованого звуку (шуму обертання) знаходиться в межах 70 дБ -102 дБ, що збігається з результатами досліджень квадратного аеротаксі, а також таксі з розташуванням гвинтів за літаковим типом. Енергія шуму обертання, що генерується, зосереджена у перших 4-5 гармоніках. Отже, запропонована у роботі модель шуму аеродинамічного походження може бути використана для вивчення шуму обертання аеротаксі квадратного типу.

Ключові слова: генерація звуку обертання аеротаксі; розрахунок характеристик звукового поля.

Петро Лук'янов – канд. фіз.-мат. наук, старш. наук. співроб., доц. каф. авіа- та ракетобудування, Національний технічний університет України «КПІ ім. Ігоря Сікорського», Київ, Україна.

Олег Душеба – магістр, асп. каф. авіа- та ракетобудування, Національний технічний університет України «КПІ ім. Ігоря Сікорського», Київ, Україна.

Petro Lukianov – Candidate of Physics and Mathematics Sciences, Senior Researcher, Associate Professor of the Department of Avia- and Rocket Constructions, National Technical University of Ukraine “Igor Sikorsky Kyiv Polytechnic Institute”, Kyiv, Ukraine,

e-mail: p.lukianov@kpi.ua, ORCID: 0000-0002-7584-1491.

Oleg Dushaba – Master of Technical Sciences, PhD student of the Department Avia- and Rocket Constructions, National Technical University of Ukraine “Igor Sikorsky Kyiv Polytechnic Institute”, Kyiv, Ukraine, e-mail: olegdushaba@gmail.com, ORCID: 0000-0002-0033-2414.